Energy & Buildings 254 (2022) 111565

Contents lists available at ScienceDirect

Energy & Buildings

journal homepage: www.elsevier.com/locate/enb

Ground characterization of building energy models

Vicente Gutiérrez González [a], Germán Ramos Ruiz [a,*], Carlos Fernández Bandera [a]

[a] Department of Building Construction, Services and Structures, School of Architecture, Universidad de Navarra, Pamplona 31010, Navarra, Spain

ARTICLE INFO

Article history:
Received 10 August 2021
Revised 7 October 2021
Accepted 8 October 2021
Available online 16 October 2021

Keywords:
Ground characterization
EnergyPlus
Building energy model
BEM
Uncertainty analysis
Energy savings

ABSTRACT

The calibration of building energy models is crucial for their use in some applications that depend on their accuracy for adequate performance, such as demand response and model predictive control (MPC). In general, energy models offer many possibilities/strategies when characterizing a construction system, and such a characterization is key when analyzing both its thermal behavior and its energy impact. This research analyzes the different ways to characterize the thermal interaction of the building energy model (BEM) with the ground, comparing conventional approaches with new approaches based on both optimization of the former and dynamic ground characterizations. Using a model adjusted to a real case study, each of the existing options are analyzed, in which a different control of the ground temperature both in terms of its temporal oscillation and its location in the building (based on thermal zones) is taken into account. Exhaustive monitoring of a real building and measuring the ground and ground floor surface temperatures have made establishing which EnergyPlus components/objects best characterize the ground-slab interaction possible, both in terms of the simplicity of modeling and the cost (economic and technical) required for each of them. As will be seen, there are objects with an excellent cost/effectiveness ratio when characterizing the ground.

1. Introduction

The use of virtual models is currently an indispensable tool when performing studies for the improvement of the products and equipment they represent. In the case of architecture, building energy models (BEM) are essential both in the initial design stages and in constructed buildings, since they provide detailed information on their energy performance in different situations and make analyzing which energy conservation measures (ECMs) are most appropriate or establishing optimal use strategies according to certain objectives (demand response (DR) or model predictive control (MPC) among others) possible. Knowing the physics of the building helps to discern in which areas an opportunity for improvement is available in order to reduce its energy consumption. This aspect is key not only at an economic level but also at an environmental level, since the energy consumption of buildings accounts for 40% of CO_2 emissions [1], being essential in the fight against climate change.

However, for all of these measures and strategies for improvement to be valid and feasible, the accuracy of the models must be high. Several international standards are available to quantify the quality of energy models, the most widely used of which are the American Society of Heating, Refrigerating and Air-Conditioning Engineers (ASHRAE) [2]; the International Performance Measurement and Verification Protocol (IPMVP) [3]; and the Federal Energy Management Program (FEMP) [4], which establish uncertainty indices that measure the accuracy of energy models, above which such models are considered to be calibrated. Table 1 shows the limits of such standards.

The process of adjusting the BEM parameters to obtain a model in which the predictions better match reality and comply with these standards is called calibration [5]. It is a rather complex process, since not only is the model intended to represent the overall (annual/monthly) consumption of the building but also, for many applications and buildings that use optimization strategies, analyzing its hourly, even the ten-minute time step consumption (e.g., in demand response strategies [6] or model predictive control strategies [7–11]), is necessary. In these cases, the number of parameters to be adjusted is large, since it includes not only the building envelope (energy demand) but also the HVAC systems (energy consumption), which includes performance curves or modes of use [12].

Strategies for obtaining calibrated BEM models can be divided into two groups: (1) manual calibrations based on iterative processes [13] (which require a great deal of experience on the part of the modeler—in fact, in Table 4.2 of the ASHRAE Guideline 14–

* Corresponding author.
E-mail addresses: vgutierrez@unav.es (V. Gutiérrez González), gramrui@unav.es (G. Ramos Ruiz), cfbandera@unav.es (C. Fernández Bandera).

https://doi.org/10.1016/j.enbuild.2021.111565
0378-7788/

Nomenclature

Q	Heat transfer through the slab (W)
Area	Slab or wall area (m^2)
Ueff	The effective heat transfer coefficient including the floor construction, the soil and the thermal resistance of the interior and exterior air films
Tair,out	Outside air temp (°C)
Tair,in	Indoor air temp (°C)
Pexp	Exposed perimeter of the slab (m)
Rsoil	Effective R-value of the soil
R film,out	Air film resistance of the outside surfaces
F-factor	The heat transfer through the floor, induced by a unit temperature difference between the outside and inside air temperature, on the per linear length of the exposed perimeter of the floor (W/m.K).
C-factor	Time rate of steady-state heat flow through unit area of the construction, induced by a unit temperature difference between the body surfaces ($W/m^2.K$)
R film,in	Air film resistance of the inside surfaces
T(z,t)	Undisturbed ground temperature as a function of time and depth
Ts	Average annual soil surface temperature (°C)
Ts	The amplitude of the soil temperature change throughout the year (°C)
α	Thermal diffusivity of the ground
θ	Phase shift, or day of minimum surface temperature
τ	Time constant (365)
$\Delta\overline{T}_{s,n}$	n-th amplitude of the soil temperature change throughout the year (°C)
θ_n	n-th phase shift, or day of minimum surface temperature

Table 1
Calibration criteria of the Federal Energy Management Program (FEMP), ASHRAE, and IPMVP.

Data type	Index	FEMP 3.0 Criteria	ASHRAE G14–2014	IPMVP
Calibration criteria				
Monthly criteria %	*NMBE*	±5	±5	±20
	CV(*RMSE*)	±15	±15	–
Hourly criteria %	*NMBE*	±10	±10	±5
	CV(*RMSE*)	±30	±30	±20

2014 [14], the authors established that, in order to perform a "*whole building calibrated simulation*", it is necessary that the "*special skills of personnel*" have "*five years computer simulation experience*") and (2) automatic calibrations [15,16]. The latter are perhaps the most widely used since they simplify the process of obtaining the parameters that make the model more similar to reality. Among them are those that use Bayesian processes [17–20], regression processes [21], metaheuristic strategies such as genetic algorithms [22,23], neural networks [24,25], or clustering and surrogate techniques [26]. The objectives of each are always the same: to select the most sensitive parameters in the simulation and to obtain their values [27,28]. In these automatic processes of obtaining calibrated models, in general, many similar solutions to the problem exist, in which the behaviors must be analyzed to select the most appropriate for the situation. In fact, once the model has undergone an adjustment or calibration process, the parameters values may not correspond to physically realistic values, losing the capacity to understand the physics behind the model [5]. This is because automatic calibration processes aim for the best fit of the model with the real data rather than its correspondence with the construction systems of the building. It must be taken into account that, in these calibration processes, sometimes, values that compensate for the errors of both the simulation software itself and the energy model are obtained for the sake of better adjustment with the measurements taken.

This research focuses on this aspect and on the suitability and adequacy of objects that characterize the energy behavior in the simulation models, in particular on the objects and strategies in charge of characterizing the interaction of the building energy model with the ground.

Building façades are perhaps the construction systems to which architects and designers pay most attention, mainly because they are responsible for the building's aesthetic, although logically—due to their large surface area—they have a greater energy contribution to the exterior. Even roofs, as expressed by Le Corbusier and Pierre Jeanneret [29] in their manifesto "*Five Points Towards a New Architecture*", are considered the "*fifth façade*" of the building: "*In general, roof gardens mean to a city the recovery of all the built-up area*". This concept, highlighted by Richard Cook [30], "*describes the potential of the urban roof-scape in terms of architecture design*". Considering slabs-on-grade foundations as the "sixth façade" does not make much sense in terms of aesthetics/design, but it does in energy terms, since as an element of the thermal envelope of spaces, it is responsible for a part of the thermal losses/gains of the building. Façades and roofs depend on the weather as an element of the outside boundary [31], while the slabs-on-grade foundations use the ground. Considering that, in general, Europe's building stock consists of single-family houses or low-rise buildings, the impact of this element on the overall consumption is high.

Of the different energy simulation software available on the market, in this research, EnergyPlus [32] is used, since it is currently one of the most widely used for performing BEMs [33]. The energy interaction of the model with the ground is so important that EnergyPlus continues developing objects to improve the accuracy when characterizing it, such as the one received in its version 8.7 in March 2017, with Kiva object. The Kiva foundation heat transfer module is a computational framework developed by Neal Kruis [34] that reduces the time needed to perform a three-dimensional heat transfer calculation using a two-dimensional simulation. This reduces the time needed to perform a simulation to seconds, obtaining a result within a mean absolute deviation of 3%. However, it is not the only object/strategy with which characterizing the ground is possible; others also allow for control of the ground temperature both in terms of its temporal thermal oscillation (monthly and time step) and by its position in the model (mono/multi-thermal zone).

Fig. 1 shows all of the approaches analyzed in this research in order to evaluate the suitability in characterizing the interaction between the ground and the building. From the conventional approaches, which include the five existing possibilities in Energy-

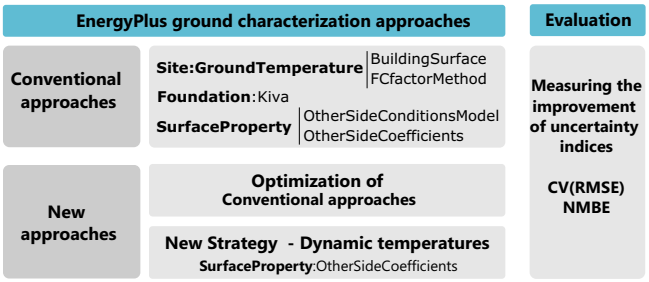

Fig. 1. Ground characterization approaches in EnergyPlus.

Plus to model the ground, to new approaches that aim to improve these characterizations. These new approaches include both genetic algorithm optimizations of the parameters defining each of the conventional approaches and new strategies that allow for more accurate calculation through the use of dynamic temperatures at the cost of increased ground data gathering. Each of these characterizations has been evaluated by measuring the resulting improvement in the uncertainty indices—CV(RMSE) and NMBE—with respect to the baseline model in which the EnergyPlus default ground characterization has been used.

The main objectives of this research are (1) to present all of the existing possibilities when characterizing the ground in BEMs using EnergyPlus; (2) to show other non-conventional approaches when modeling the ground, one of which—as will be seen in Section 2—allows us to reproduce the thermal waveform both by time step (ten-minute intervals and hourly) and by thermal zone; and (3) to evaluate and classify them by measuring the thermal offset between the model and the real building using the CV(RMSE) and NMBE uncertainty indices.

This research completes and concludes a previous work presented at the 16th IBPSA International Conference and Exhibition, held in Rome in 2019 [35]. It is organized as follows: Section 2 describes the methodology used in which each of the EnergyPlus components related to the ground is analyzed, emphasizing the heat transfer; Section 3 explains the case study and the tests that have been performed for each of the components; Section 4 shows the results and discusses the findings; and finally, Section 5 provides the conclusions.

2. Methodology

This section explains the approaches used to find out which EnergyPlus object/strategy best characterizes the interaction of the ground with the building. For this purpose, the study is based on a building previously adjusted and evaluated according to the quality standards established by ASHRAE guideline 14 for calibrated buildings (see Section 3), in which the default EnergyPlus configuration for ground characterization, the object ("*Site: GroundTemperature: BuildingSurface*") [36], has been used. This object sets a ground temperature of 18 °C throughout the year, the same as that for all surfaces in contact with the ground. As one can expect, this object, with the default setting, is one of the worst ground characterizations.

Then, both an adjustment of this first component and a substitution by others is performed, measuring the deviation of the model (predicted vs. measured temperature) in each approach using the uncertainty indices normalized mean bias error (NMBE) and coefficient of variation of root mean square error CV (RMSE) [37,38], so that which of them improves the results by increasing the accuracy of the model can be established.

As shown in Fig. 1, five objects for ground characterization are analyzed using two different approaches: conventional ones and new approaches. The latter include two methods: optimizations by genetic algorithms of the conventional approaches and reproduction of the dynamic ground thermal wave in the simulation model thanks to temperature measurements of both the ground and the inside face of the ground floors. Each of these EnergyPlus objects is classified according to its boundary conditions: "*Site: GroundTemperature*", "*Foundation*", and "*SurfaceProperty*".

Fig. 2 shows the versatility of each of them, focusing on three fundamental aspects: (1) the frequency of the temperatures, directly related to the possibility of having a detailed thermal waveform; (2) the discrimination by thermal zone, which establishes whether the temperatures obtained can be differentiated by the thermal zone; and (3) the control of the component, which establishes whether such control goes beyond the object's own variables. It seems logical to establish that more control of the ground object produces better results; however, in order to characterize it correctly, having the information that the object needs, information that sometimes is not available in a simple way, is necessary. In addition, evaluating whether the complexity of using an object that gives more control of the ground has an effect of the same magnitude on the results obtained is necessary.

The following is a brief description of the fundamentals of each:

- **Site:GroundTemperature:BuildingSurface**: This object performs a heat transfer between the ground and the opaque elements at ground level by means of one-dimensional (1D) calculations, which speeds up calculation times. It applies the monthly ground temperature to the outside surface of the exposed face, the one in contact with the ground. The EnergyPlus "*input output reference*" [36] recommends not using the temperatures from the weather files (*.epw) in which there are monthly temperatures at depths of −0.5 m, −2.0 m, and −4.0 m, as they are considered too extreme, being recommended for situations where the model has geothermal wells. Instead, it advises using the Slab/Basement program (Utilities/EnergyPlus) to calculate monthly average temperatures according to the ground and the slab/basement characteristics or even using a default value of 2 °C less than the average indoor space temperature as the monthly average ground temperature.
- **Site:GroundTemperature:FCfactorMethod**: This object calculates the heat transfer that occurs in the slab-on-grade of the building, creating a similar construction to the existing one with the same U-factor. It consists only of a concrete layer and an insulation layer, being constructions based on C or F factor [36]. The ground temperatures are close to monthly outdoor air temperatures delayed by three months, using the information from the weather file (*.epw). In case they are not defined, the program selects the existing ones at a depth of −0.5 m. Once all parameters are defined, the heat transfer through the slab-on-grade is calculated using the following equation:

$$Q = Area \cdot U_{eff} \cdot \left(T_{air,out} - T_{air,in}\right) = \left(T_{air,out} - T_{air,in}\right) \cdot \left(P_{exp} \cdot F - factor\right) \quad (1)$$

Additionally, the heat transfer through the walls is calculated using the following equation:

$$Q = Area \cdot 1/\left((1/C - factor + R_{soil}) + R_{film,out} + R_{film,in}\right) \cdot \left(T_{air,out} - T_{air,in}\right) \quad (2)$$

- **Foundation:Kiva**: Implemented in EnergyPlus 8.7, it is a tool that calculates ground heat transfer in a multidimensional way time step by time step, considerably reducing computational times. The ground temperatures are not defined but are calculated based on the characteristics of the ground and foundation surfaces and by taking into account the weather data and the zone temperatures of the model.

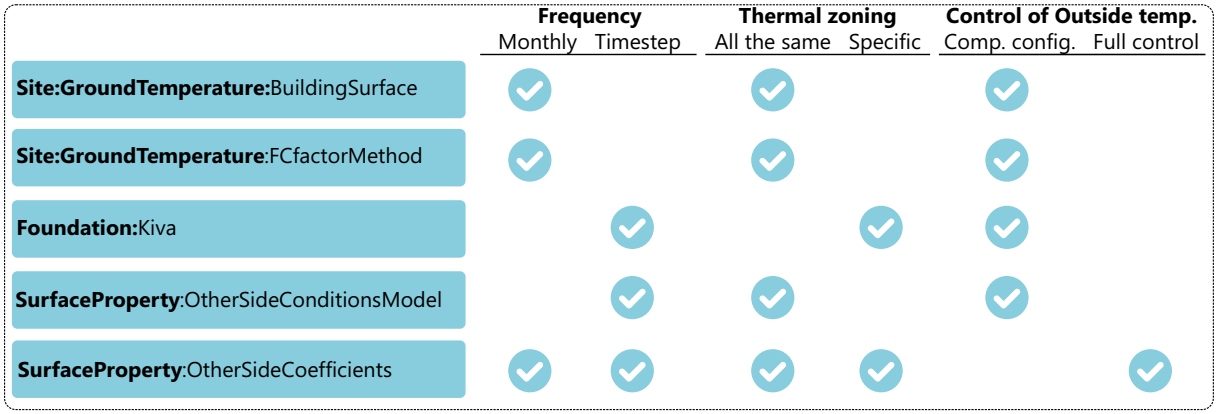

Fig. 2. EnergyPlus objects to characterize the ground-building interaction.

Knowing the footprint shape, area, and exposed perimeter, Kiva performs a two-dimensional approximation method, which subsequently automatically discretizes into rectangular cells with a "minimum cell dimension" and "maximum cell growth coefficient". The alternating direction implicit (ADI) finite difference time stepping scheme is used to solve the discretized partial differential equations that, as Kruis and Krarti [39] demonstrates, provides relatively fast calculations with stable results.

- **SurfaceProperty:OtherSideConditionsModel**: It is defined at the surface level as an outside boundary condition. In this case, the boundary condition is a ground model that is considered "*undisturbed*", that is, annual ground temperatures of stable periodicity. Three methodologies can be used to calculate it: "*FiniteDifference*"; "*Kusuda-Achenbach*" [40], and "*Xing*" [41]. In all of them, detailed temperatures are obtained by a time step; however, their control does not go beyond the definition of the object.
  FiniteDifference: The FiniteDifference calculation methodology estimates a stable annual ground temperature ("*undisturbed*") using a one-dimensional finite-difference heat transfer model. This temperature relies on the weather file but does not take into account vegetative layers, snow, or different factors not covered by the weather that can affect the ground temperature.
  KusudaAchenbach: For the determination of heat transfer between the ground and the thermal zone under study, the model uses the correlation created by Kusuda and Achenbach [40] to define its temperature. It requires the average ground surface temperature, its amplitude, and the day of minimum surface temperature within the analyzed period, as can be seen in the equation:

$$T(z,t) = \overline{T}_s - \Delta\overline{T}_s \cdot e^{-z\cdot\sqrt{\frac{\pi}{\alpha\cdot\tau}}} \cdot \cos\left(\frac{2\pi t}{\tau} - \theta\right) \tag{3}$$

  Xing: This object uses the correlation developed by Xing in 2014 for the calculation of the ground temperature [41]. The data required for its calculation largely coincide with those used by Kusuda and Achenbach, although Xing proposes to individualize the results by adding up the different time steps that make up the period analyzed, as can be recognized in its equation:

$$T(z,t) = \overline{T}_s - \sum_{n=1}^{2}\Delta\overline{T}_{s,n} \cdot e^{-z\cdot\sqrt{\frac{n\pi}{\alpha\tau}}} \cdot \cos\left[\frac{2\pi n}{\tau}(t-\theta_n) - z\sqrt{\frac{n\pi}{\alpha\tau}}\right] \tag{4}$$

- **SurfaceProperty:OtherSideCoefficients**: This object is very similar to *Site:Ground Temperature:BuildingSurface*. It allows us to control the temperature of the outer plane of a surface directly. In this way, it is possible both to use any time interval and to apply it to any surface or group of surfaces, making the behavior of each thermal zone independent. This total control entails a higher definition as more data are needed. Through this object, heat transfer is simulated by *conduction transfer functions* that eliminate the need to know the temperature and heat fluxes within surfaces, although they become progressively more unstable as the time interval decreases [42]. This object, conceived by EnergyPlus to allow for the use of monthly temperatures by thermal zones, has been used in this research to reproduce the dynamic thermal wave of the ground, thanks to the monitoring carried out both on the ground and on the interior surfaces of the spaces.

After reviewing the fundamentals of each of the EnergyPlus objects, Sections 3 and A detail the configurations considered in each for all approaches, conventional and new, including the settings used for both the optimizations and the implementation of the dynamic thermal wave per thermal zone.

3. Case study

To perform this study, the office building of the School of Architecture of the University of Navarra was chosen. Designed by Rafael Echaide, Carlos Sobrini, and Eugenio Aguinaga, this building won the "*National Brick Architecture Award*" in 1978. As a single-story building for administrative use, it has an approximate area of $755m^2$. It has a porticoed structure of reinforced concrete, brick façades and double-glazed windows without thermal bridge break.

As can be seen in Fig. 3, the building has a compact shape with a large roof and floor area, reaching 80% of the building envelope (40% each). The slab-on-grade in contact with the ground is composed from the outside to the inside by a reinforced concrete slab on a layer of gravel, a leveling layer, mortar, and terrazzo. Due to its large exchange surface and the absence of insulation, the influence of the ground characterization on the simulation results is considerable.

The building energy model developed with EnergyPlus (version 9.5) has 25 thermal zones, as shown in Fig. 4, and was adjusted to the real building following the methodologies developed by Bandera and Ramos [43] and by Gutierrez et al. [44]. The weather file used was created using the meteorological data obtained from a weather station placed on the roof of the building.

Fig. 3. Office building, School of Architecture (University of Navarra) [35].

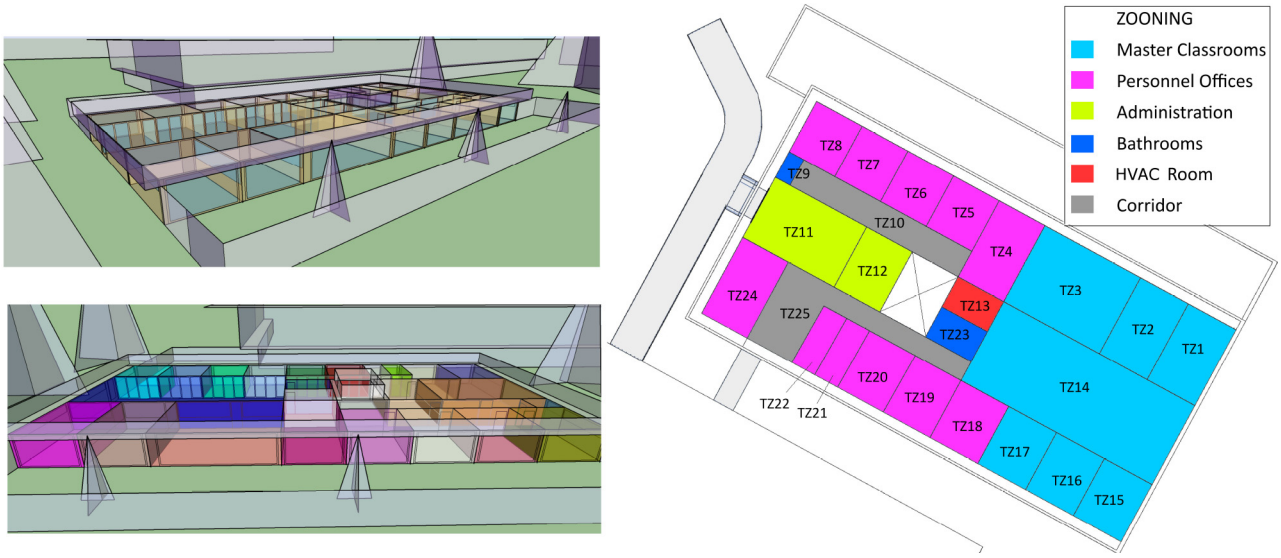

Fig. 4. Building energy model showing the thermal zoning of the Office building, School of Architecture (University of Navarra) [35].

The results obtained after carrying out the adjustment process were an *NMBE* of 4.33% and a *CV*(*RMSE*) of 4.78%, both within the ranges of ASHRAE, FEMP, and IPMVP standards (see Table 1), corresponding to a three-month period (May–July) of 2017 using the temperatures measured in each thermal zone with a ten-minute time step.

The configurations used in the simulations for the different approaches used for ground characterization are described below:

3.1. EnergyPlus conventional approaches for ground characterization

Fig. 5 shows a summary of the configurations used in each of the simulations for the EnergyPlus conventional approaches. In bold, the tag used was identified in the Results section (see Table 2).

A brief description of each configuration is shown below:

Site:GroundTemperature: BuildingSurface

- **Baseline model**: The 12 months have a uniform ground temperature equal to 18 °C.
- **EPW ground temp**: Three models are performed, each with temperatures from the weather file (*.epw) corresponding to depths of −0.5 m, −2.0 m, and −4.0 m.
- **EPW ground temp ± 10**: Starting from the previous configuration, a variation between −10 °C and +10 °C is applied in 0.5 °C intervals.
- **Average TZ**: The monthly average temperature (weighted by surface) of all the thermal zones is calculated, subtracting −0.5, −1.0, −1.5, −2.0, −2.5, and −3 °C from all of them.

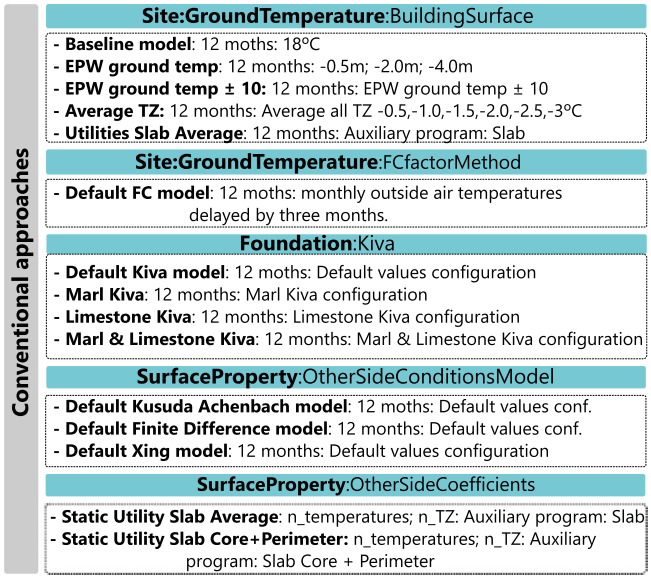

Fig. 5. EnergyPlus conventional approaches for ground characterization.

- **Utilities Slab Average**: The EnergyPlus Utilities Slab tool has been used to obtain the ground temperature values according to the slab and ground characteristics. From this tool, an aver-

Table 2
All simulations results in terms of *CV*(*RMSE*), *NMBE*, and *MAE*.

Model	Outside Boundary Condition	*CV*(*RMSE*) %	*NMBE* %	*MAE* °C
Dynamic Ground Temp	Other Side Coefficients	1.50%	0.26%	**0.27**
Optimized Kiva	Foundation	1.58%	−0.36%	**0.25**
Static Utility Slab Average	Other Side Coefficients	1.61%	0.12%	**0.28**
Utilities Slab Average	Ground	1.61%	0.12%	**0.28**
Average TZ – 1.5 °C	Ground	1.62%	−0.11%	**0.28**
Average TZ – 2.0 °C	Ground	1.64%	0.59%	**0.31**
Dynamic Interior Surface Temp + Value (-2 + 3 °C)	Other Side Coefficients	1.73%	0.00%	**0.30**
Static Utility Slab Core + Perimeter	Other Side Coefficients	1.79%	0.95%	**0.35**
Optimized Finite Difference model	Other Side Conditions Model	1.81%	0.20%	**0.33**
Marl Kiva	Foundation	1.82%	−0.81%	**0.28**
Average TZ – 1.0 °C	Ground	1.90%	−0.82%	**0.30**
Marl & Limestone Kiva	Foundation	1.90%	−0.92%	**0.29**
Optimized Xing model	Other Side Conditions Model	1.92%	0.52%	**0.36**
Average TZ – 2.5 °C	Ground	1.96%	1.29%	**0.39**
Limestone Kiva	Foundation	2.03%	−1.08%	**0.31**
Optimized Kusuda Achenbach model	Other Side Conditions Model	2.05%	0.23%	**0.38**
Optimized Fixed Temp	Other Side Coefficients	2.16%	1.21%	**0.40**
Average TZ – 0.5 °C	Ground	2.37%	−1.52%	**0.39**
Average TZ – 3.0 °C	Ground	2.44%	1.99%	**0.50**
Default Finite Difference model	Other Side Conditions Model	2.48%	−1.73%	**0.43**
EPW ground temp ± 10	Ground	2.56%	0.70%	**0.50**
Dynamic Interior Surface Temp	Other Side Coefficients	2.79%	2.51%	0.58
Optimized FC model	FC factor Method	2.83%	−1.39%	**0.46**
Default Kiva model	Foundation	2.85%	−1.91%	**0.45**
Default Xing model	Other Side Conditions Model	3.41%	2.91%	0.67
Default Kusuda Achenbach model	Other Side Conditions Model	3.54%	3.04%	0.70
Default FC model	FC factor Method	3.77%	−2.62%	0.63
Baseline model	**Ground**	4.79%	4.34%	0.98
EPW ground temp −0.5 m	Ground	10.64%	9.91%	2.21
EPW ground temp −2.0 m	Ground	12.12%	11.81%	2.64
EPW ground temp −4.0 m	Ground	12.75%	12.48%	2.79

age temperature as well as a core and a perimeter temperature (see Table 7 of A) are obtained. These twelve average temperatures are used in this option.

Site:GroundTemperature: FCfactorMethod

- **Default FC model**: In this case, the outdoor temperatures of the weather file (*.epw) delayed by three months have been used as ground temperatures.

Foundation: Kiva

- **Default Kiva model**: The model is simulated with the default data provided by EnergyPlus when the object is activated.
- **Marl Kiva**; **Limestone Kiva**; **Marl and Limestone Kiva**: The ground found during the construction of the building is a "tufa". This ground is a mixture of marls and limestones that weathered in contact with the outside air. For the definition of this object three simulations were conducted, using the specific values of marls, limestones, and an average of both following the values that are shown in the Spanish Technical Building Code [45].

Table 7
EnergyPlus Utility: Slab model configuration.

	Static Utility Slab		
	Average Temp. °C	Perimeter Temp. °C	Core Temp. °C
January	18.43	16.32	19.25
February	18.86	16.67	19.72
March	18.6	16.65	19.35
April	19.04	17.34	19.7
May	20.15	18.69	20.72
June	21.51	20.17	22.03
July	21.82	20.44	22.36
August	21.88	20.55	22.4
September	20.43	19.02	20.98
October	19.49	18.05	20.05
November	19.05	17.68	19.59
December	17.9	16.81	18.32

SurfaceProperty: OtherSideConditionsModel

In the cases "**Default Kusuda Achenbach Model**, "**Default Finite Difference Model**", and "**Default Xing Model**", the default object settings are used.

SurfaceProperty: OtherSideCoefficients

As seen in Section 2, the "*OtherSideCoefficients*" is the most versatile object for setting the boundary conditions of any surface in EnergyPlus. This object is not intended to be a ground object itself; however, due to its great versatility, it can be used as such, compensating for the shortcomings of the other specific objects of EnergyPlus. Therefore, as will be seen, the number and configuration of the strategies used is quite varied.

One of the options to be analyzed is the ability of this object to specify ground temperatures by thermal zone. Therefore, as in the "**Utilities Slab Average**" option, the Utilities Slab tool of EnergyPlus has been used to obtain the average, core, and perimeter temperatures depending on the characteristics of the ground and the foundation, obtaining the "**Static Utility Slab Average**" and "**Static Utility Slab Core + Perimeter**" simulations. It can be expected that the results of "**Utilities Slab Average**" and "**Static Utility Slab Average**" should be the same, since the same temperatures have been used (see Table 2).

3.2. Optimization of EnergyPlus conventional approaches for ground characterization

All of the options discussed in the previous subsection can be optimized by modifying their values according to the temperature ranges, the properties of different types of grounds, or the settings

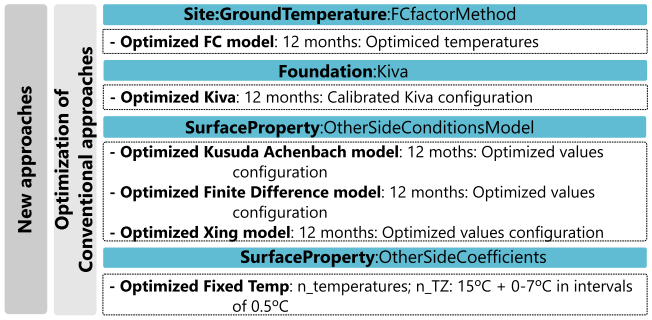

Fig. 6. Optimized EnergyPlus new approaches for ground characterization.

of individual objects. In this research, optimizations have been performed using the JEplus + EA software [46], which uses the Non-Dominated Sorting Genetic Algorithm-II (NSGA-II) [47]. The main characteristics of this algorithm are that it uses the principle of elitism of the generated solutions, ranks them according to a non-dominance criterion, and has operators that preserve the diversity of the solutions. This allows the algorithm to converge quickly to optimal solutions, avoiding falling into local minima. Fig. 6 shows a summary of the configurations used in each of the simulations, highlighting the tag used to be identified in the global results in bold (see Table 2).

Thus, we have the following optimizations: "**Optimized FC model**", which uses the default ranges of the FC models; "**Optimized Kiva**", which takes into account the properties of marls and limestones; "**Optimized Kusuda Achenbach Model**", "**Optimized Finite Difference Model**", and "**Optimized Xing Model**", which uses the ranges of each of the model types; and "**Optimized Fixed Temp**", in which the temperature in contact with the slab-on-grade is varied by a thermal zone starting from a fixed value of 15 °C by adding values in 0.5 °C intervals between 0 and 7 °C.

All of the values and ranges chosen in these simulations can be found in Tables 4, 5, 6, and 8 of A.

3.3. New EnergyPlus strategies for ground characterization

Finally, as a new strategy for ground characterization in EnergyPlus, the dynamic potential of the object "*SurfaceProperty:OtherSideCoefficients*" is used. This new approach leverages the measurements made during building monitoring of both the interior surfaces of the zones and the temperature sensors placed on the ground. With all of this, three different strategies for ground characterization are performed. Fig. 7 shows a summary of the configurations used in each of the simulations, highlighting the tag used to be identified in the global results in bold (see Table 2).

The following is a brief description of each strategies:

- **Dynamic Interior Surface Temp**: The temperature of the exterior face of the slab is replaced by the interior surface temperature of the floor measured by thermal zone.
- **Dynamic Interior Surface Temp + Value (-2 + 3 °C)**: Based on the previous model, an optimization is performed using genetic algorithms, as in the previous subsection. This optimization consists of adding intervals of 0.5 °C between −2 and 3 °C to the interior surface temperature of the floor by thermal zone.
- **Dynamic Ground Temp**: The external face temperature of the slab by the thermal zone are replaced by those provided by the sensors placed in the ground of the building. Fig. 8 shows one of the sensors used.

All of the values and ranges chosen in the simulations using this object can be found in Table 8 of A.

Table 5
Object: Foundation:Kiva. Simulation settings.

Kiva Method	Default Kiva model	Optimized Kiva
Foundation:kiva		
Soil Conductivity	1.73	from 0.50 to 2.50 every 0.10
Soil Density	1842	from 1200 to 2800 every 100
Soil Specific Heat	419	from 200 to 1500 every 100
Ground Solar Absorptivity	0.9	from 0.10 to 0.99 every 0.10
Ground Thermal Absorptivity	0.9	from 0.10 to 0.99 every 0.10
Ground Surface Roughness	0.03	from 0.005 to 0.03 every 0.005
Far-Field Width	40	from 16.50 to 20 every 0.50
Foundation:kiva:Settings		
Wall Height Above Grade	–	0.2
Footing Depth	–	0.3

4. Results and discussion

Table 2 shows the results obtained from the different strategies used to characterize the ground. The table is organized as follows: the first column shows the tag used to describe each simulation where the gray shaded cells highlight those corresponding to the new approaches; the second column describes the outside boundary conditions on which each of the simulations depend, so that it is possible to observe which of them performs best in characterizing the building-ground interaction; the third and fourth columns show the uncertainty indices $CV(RMSE)$ and $NMBE$, calculated

Table 4
Object: GroundTemperature:FCfactorMethod. Simulation settings.

FC factor Method	Default FC model	Optimized FC model
Site:GroundTemperature:FCfactorMethod		
January	6.4	from 5.50 to 11.50 every 0.50
February	5.72	from 4.50 to 9.50 every 0.50
March	6.93	from 5.50 to 9.00 every 0.50
April	8.82	from 7.00 to 10.50 every 0.50
May	13.77	from 10.50 to 14.00 every 0.50
June	17.59	from 14.00 to 17.50 every 0.50
July	20.17	from 16.50 to 20.00 every 0.50
August	20.95	from 17.00 to 22.00 every 0.50
September	19.62	from 16.00 to 23.00 every 0.50
October	16.65	from 13.50 to 21.50 every 0.50
November	12.69	from 10.50 to 18.50 every 0.50
December	9.01	from 7.50 to 14.50 every 0.50

Table 6
Object: OtherSideConditionsModel. Simulation settings.

	KusudaAchenbach		FiniteDifference		Xing	
	Default	Optimized	Default	Optimized	Default	Optimized
Site:GroundTemperature:Undisturbed						
Soil Conductivity (W/m-K)	1.5	from 0.5 to 2.5 every 0.1	1.5	from 0.5 to 2.5 every 0.1	1.5	from 0.5 to 2.5 every 0.1
Soil Density (kg/m^3)	2800	from 1600 to 3400 every 100	2800	from 1600 to 3400 every 100	2800	from 1600 to 3400 every 100
Soil Specific Heat (J/kg-K)	850	from 250 to 900 every 50	850	from 250 to 900 every 50	850	from 250 to 900 every 50
Average Soil Surface Temperature (°C)	13.6	from 12.5 to 17.5 every 0.5	—	—	13.6	from 12.5 to 17.5 every 0.5
Average Amplitude of Surface Temperature (delta °C)	7.9	from 5.5 to 11 every 0.5	—	—	—	—
Phase Shift of Minimum Surface Temperature (days)	26	from 24 to 35 every 1	—		—	—
Soil Moisture Content Volume Fraction (%)	—	—	30	from 10 to 50 every 5	—	—
Soil Moisture Content Volume Fraction at Saturation (%)	—	—	50	from 30 to 70 every 5	—	—
Evapotranspiration Ground Cover Parameter (dimensionless)	—	—	0.4	from 0.1 to 1.4 every 0.2	—	—
Soil Surface Temperature Amplitude 1 (delta °C)	—	—	—	—	7.9	from 5.5 to 11 every 0.5
Soil Surface Temperature Amplitude 2 (delta °C)	—	—	—	—	1.4	from −1 to 2 every 0.5
Phase Shift of Temperature Amplitude 1 (days)	—	—	—	—	26	from 24 to 35 every 1
Phase Shift of Temperature Amplitude 2 (days)	—	—	—	—	−33	from −40 to 10 every 10
GroundDomain:Slab						
Ground Domain Depth (m)	10	from 4 to 12 every 1	10	from 4 to 12 every 1	10	from 4 to 12 every 1
Perimeter Offset (m)	5	from 4 to 12 every 2	5	from 4 to 12 every 2	5	from 4 to 12 every 2
Soil Conductivity (W/m-K)	1.5	from 0.50 to 2.50 every 0.10	1.5	from 0.5 to 2.5 every 0.1	1.5	from 0.5 to 2.5 every 0.1
Soil Density (kg/m^3)	2800	from 1600 to 3400 every 100	2800	from 1600 to 3400 every 100	2800	from 1600 to 3400 every 100
Soil Specific Heat (J/kg-K)	850	from 250 to 900 every 50	850	from 250 to 900 every 50	850	from 250 to 900 every 50
Soil Moisture Content Volume Fraction (%)	30	from 10 to 50 every 5	30	from 10 to 50 every 5	30	from 10 to 50 every 5
Soil Moisture Content Volume Fraction at Saturation (%)	50	from 30 to 70 every 5	50	from 30 to 70 every 5	50	from 30 to 70 every 5
Evapotranspiration Ground Cover Parameter	0.4	from 0.1 to 1.4 every 0.2	0.4	from 0.1 to 1.4 every 0.2	0.4	from 0.1 to 1.4 every 0.2

Table 8
Object: OtherSideCoefficients. Simulation settings.

	OtherSideCoefficients	
	Thermal zones	Temperatures
Optimized Fixed Temp	from TZ01 to TZ25	15 °C + (from 0 °C to 7 °C every 0.5 °C)
Dynamic Interior Surface Temp	from TZ01 to TZ25	Internal surface temperature of the slab
Dynamic Interior Surface Temp + Value (−2 + 3°C)	from TZ01 to TZ25	Internal surface temp. of the slab + (from −2 °C to 3 °C every 0.5 °C)
Dynamic Ground Temp	from TZ01 to TZ25	External surface temperature of the slab

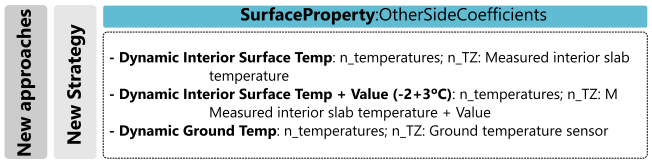

Fig. 7. New EnergyPlus strategies for ground characterization.

using the ten-minutal indoor temperatures of the thermal zones of the model weighted by their areas; and the fifth column shows a third uncertainty index, the Mean Absolute Error (*MAE*) obtained taking into account the same temperatures as the previous indices. *MAE* index is not used by the standards, but it is a very useful index since it measures the average difference between two values (in this case: the temperatures), establishing a quantitative scale of values, easier to understand than the qualitative values *NMBE* and *CV*(*RMSE*). In fact, for certain applications that require measuring aspects such as user comfort, it is advised that the MAE does not exceed 0.5 °C (which is usually the tolerance of the temperature sensor). MAE values lower than 0.5 °C are highlighted in bold. Table 2 has been sorted from lowest to highest according to the uncertainty index *CV*(*RMSE*).

Table 2 shows the results obtained from the different strategies used to characterize the ground. The table is organized as follows: the first column shows the tag used to describe each simulation where the gray shaded cells highlight those corresponding to the new approaches; the second column describes the outside boundary conditions on which each of the simulations depend, so that it is possible to observe which of them performs best in characterizing the building-ground interaction; the third and fourth columns show the uncertainty indices *CV*(*RMSE*) and *NMBE*, calculated using the ten-minutal indoor temperatures of the thermal zones of the model weighted by their areas; and the fifth column shows a third uncertainty index, the Mean Absolute Error (*MAE*) obtained when taking into account the same temperatures as the previous indices. The *MAE* index is not used by the standards, but it is a very useful index since it measures the average difference between two values (in this case: the temperatures), establishing a quantitative scale of values, easier to understand than the qualitative values *NMBE* and *CV*(*RMSE*). In fact, for certain applications that require measuring aspects such as user comfort, it is advised that the MAE does not exceed 0.5 °C (which is usually the tolerance of the temperature sensor). MAE values lower than 0.5 °C are highlighted in bold. Table 2 has been sorted from lowest to highest according to the uncertainty index *CV*(*RMSE*).

The first thing to highlight is the difference between the model that best characterizes the ground ("*OtherSideCoefficients: Dynamic Ground Temp*") and the baseline model. Although the baseline model has been subjected to an adjustment process obtaining good uncertainty indices, the difference in *CV*(*RMSE*) with the model that best characterizes the ground is almost 3.3%, with a reduction

Fig. 8. ensors used to measure the interior and exterior surface temperatures of the slab in contact with the ground.

in *MAE* of 0.71 °C. This temperature reduction is important, considering that the "*baseline model*" is an adjusted model, so that reducing these uncertainty indices is usually complex as all parameters are already tuned, in this case, all except the ground. This highlights the great influence of the ground in this model and the importance of using a proper object for its characterization. It is noteworthy that this solution—"*OtherSideCoefficients: Dynamic Ground Temp*"—entails the installation of sensors in the building's subsoil and implies investments or easement that may be difficult to execute or assume in all of the buildings. This disadvantage is offset by the fact that knowing the composition of the ground is not necessary.

Another point to highlight is that the worst models obtained are those that have used the "*GroundTemperature:BuildingSurface*" object when taking into account the ground temperatures of the weather file (*.epw), as the EnergyPlus documentation warns, being even worse than the baseline model, which has an object with a uniform temperature of 18 °C.

In general, models that use the "*other side coefficients*" or "*other side conditions model*" as an outside boundary condition have a better behavior than the others. This could be due to the fact that these objects use temperatures for which the interval is the "*time step*" rather than monthly values. However, there are models of "*Ground Temp Building Surface*" with very good behaviors, such as those that consider the average indoor temperatures of all thermal zones −1.5 °C and −2.0 °C.

The same applies for those that use the EnergyPlus "*Slab*" utility that calculates the average, core, and perimeter temperatures of the slab-on-grade as a function of the ground characteristics. This last characterization is very easy to implement, and the results are very close to the "*Dynamic Ground Temp*".

Finally, it should be noted that the "*Foundation:Kiva*" object has a high sensitivity, which has produced a large spread of its results. In general, the values that define the ground composition (density, conductivity, and specific heat, among others) are within a range that makes it difficult to define them correctly due to the heterogeneity of the ground. Therefore, performing an optimization in search of the best values is advisable ("*Optimized Kiva*"), which makes its use more complex compared with other more cost-effective strategies.

5. Conclusion

The main objectives of this paper are to show all of the *conventional approaches* to characterize the ground in EnergyPlus, to present *new approaches* that offer an alternative solution to this characterization, and to perform a quantitative evaluation of both to determine which of them achieves a better fit with the real data of the building under study.

As weather is one of the most influential aspects when calibrating the façades and roofs of an energy model, so is the ground for the elements that are in contact with it (slab-on-grade or foundations). Therefore, it is a fundamental part to take into account in any building calibration or adjustment process.

The office building of the School of Architecture of the University of Navarra was used for this research. The composition of the slab-on-grade foundation—without insulation—and the shape of the building—with 40% of the total exposed surface in contact with the ground—implies that the characterization of the ground–building interaction becomes decisive when obtaining a good model adjusted to reality.

After analyzing all possible objects and strategies to characterize the ground–building interaction using EnergyPlus, the following can be concluded:

- The ground is a key element in the calibration or adjustment process of an energy model; taking it into account allows the BEM to better match the real data. This research uses a BEM with the default EnergyPlus ground characterization, which after a deep study of the different possibilities, has decreased its CV(RMSE) from 4.79% to 1.50% with the best strategy.
- It seems logical that, the closer the model resembles the constructive reality, the better the results will be. This characterization is sometimes not straightforward because it requires a large amount of data, which sometimes is not easy to obtain or is complex to implement. In this case, the model that best represents reality is the "*Dynamic Ground Temp*". However, in order to carry it out, placing sensors in the ground is necessary, which under a cost/effectiveness criterion, is not feasible since other options offer similar results regarding the energy behavior of the ground–building interaction that are easier to perform. However, one of its great advantages is that knowing the characteristics of the ground is not necessary in order to produce successful results.
- From all of the results obtained, there are two solutions more cost-effective than the "*Dynamic Ground Temp*": the "*Static Utility Slab Average*" and the "*Average TZ −1.5 °C*". The former achieves a $CV(RMSE)$ of 1.61 %, while the latter achieves 1.62 %. The "*Average TZ −1.5 °C*" model only needs the interior temperatures of the thermal zones, while the "*Static Utility Slab*" model only needs the EnergyPlus slab auxiliary program to calculate the ground temperatures, in this case, using the average instead of the core and perimeter options. The first option is considered the most cost-effective, as the EnergyPlus slab utility setup is relatively straightforward and the results are similar to those obtained using "*Dynamic Ground Temp*".
- At the same time, the results obtained by the Kiva object should be highlighted. The "*Optimized Kiva*" is in second place, achieving a $CV(RMSE)$ of 1.58%. The sensitivity of this object is a noteworthy aspect. It goes from the 2.85% $CV(RMSE)$ obtained by the "*Default kiva model*" to the 1.58% achieved by the optimized model. In order to run this object properly, incorporating the ground temperatures into the model is not necessary, but incorporating its characteristics is. However, grounds are not homo-

Table 3
Object: GroundTemperature:BuildingSurface. Simulation settings.

Ground Temperature:Building Surface	Jan.	Feb.	Mar.	Apr.	May	June	July	Aug.	Sept.	Oct.	Nov.	Dec.
Site:GroundTemperature:BuildingSurface												
Baseline model	18.00	18.00	18.00	18.00	18.00	18.00	18.00	18.00	18.00	18.00	18.00	18.00
Average thermal zone temp. −0.5 °C	19.59	20.03	20.05	20.03	21.35	22.90	22.88	22.79	20.70	19.80	19.43	17.82
Average thermal zone temp. −1.0 °C	19.09	19.53	19.55	19.53	20.85	22.40	22.38	22.29	20.20	19.30	18.93	17.32
Average thermal zone temp. −1.5 °C	18.59	19.03	19.05	19.03	20.35	21.90	21.88	21.79	19.70	18.80	18.43	16.82
Average thermal zone temp. −2.0 °C	18.09	18.53	18.55	18.53	19.85	21.40	21.38	21.29	19.20	18.30	17.93	16.32
Average thermal zone temp. −2.5 °C	17.59	18.03	18.05	18.03	19.35	20.90	20.88	20.79	18.70	17.80	17.43	15.82
Average thermal zone temp. −3.0 °C	17.09	17.53	17.55	17.53	18.85	20.40	20.38	20.29	18.20	17.30	16.93	15.32
Weather ground temp. at −0.5 m.	8.26	5.21	4.39	5.10	9.22	13.83	18.16	21.30	22.22	20.74	17.19	12.71
Weather ground temp. at −2.0 m.	11.00	8.15	6.79	6.74	8.91	12.06	15.45	18.36	19.86	19.58	17.58	14.50
Weather ground temp. at −4.0 m.	12.79	10.57	9.21	8.79	9.60	11.43	13.71	15.95	17.45	17.81	16.95	15.15

geneous, so to obtain optimal results, performing an optimization process is necessary, as seen in this study, which makes it complex to use.

By analyzing the results of conventional and new approaches, evaluating the influence of the ground on the BEMs was possible, in particular in those models with a large exchange surface in contact with the ground. Future research should check if the results obtained are similar for buildings in other locations, climates zones and different construction systems, even after an energy conservation measure (ECM) has been realized in the building.

Knowledge of the different options presented in this research to characterize the ground and its evaluation in a real test site can help in obtaining high-quality calibrated or adjusted BEMs, providing suitable references when addressing their definition in the building energy modeling process.

Funding

The data used in this research were obtained thanks to the funds received from a research project granted by the Government of Navarre (SYMMETRI—"*smart campus: electro-thermal microgrid*"), and the analysis of the influence of ground interactions with the building during the process of adjusting a BEM with real data was possible thanks to funding from the Government of Navarra in the framework of the project "*From BIM to BEM: B&B*" (Ref. 0011-1365-2020-000227).

Declaration of Competing Interest

The authors declare that they have no known competing financial interests or personal relationships that could have appeared to influence the work reported in this paper.

Acknowledgements

We thank the School of Architecture of the University of Navarra, in particular, the people who work in the office building that is the subject of this work, for allowing us to place the sensors necessary to carry out the study.

Appendix A. Tables with simulation configurations

The following tables (Tables 3–8) show all of the values and ranges for each of the configurations of the different simulations performed in this research. The objective is to show the degree of complexity of each of the different options and strategies when optimally characterizing the ground–building interaction in energy terms.

References

[1] T. Abergel, J. Dulac, I. Hamilton, M. Jordan, A. Pradeep, Global status report for buildings and construction-towards a zero-emissions, Efficient Resilient Build. Constr. Sector (2019)..
[2] A.G. Ashrae, Guideline 14–2014: Measurement of energy and demand savings, ASHRAE, Atlanta, 2014.
[3] I. Committee, et al., International performance measurement and verification protocol: Concepts and options for determining energy and water savings, volume i, Tech. rep., National Renewable Energy Lab., Golden, CO (US) (2001)..
[4] L. Webster, J. Bradford, D. Sartor, J. Shonder, E. Atkin, S. Dunnivant, D. Frank, E. Franconi, D. Jump, S. Schiller, et al., M&v guidelines: measurement and verification for performance-based contracts, Tech. rep., Version 4.0, Technical Report (2015)..
[5] K.A. Ohlsson, T. Olofsson, Benchmarking the practice of validation and uncertainty analysis of building energy models, Renew. Sustain. Energy Rev. 142 (2021), https://doi.org/10.1016/j.rser.2021.110842 110842.
[6] J. Vuelvas, F. Ruiz, G. Gruosso, Limiting gaming opportunities on incentive-based demand response programs, Appl. Energy 225 (2018) 668–681, https://doi.org/10.1016/j.apenergy.2018.05.050.
[7] V. Harish, A. Kumar, Reduced order modeling and parameter identification of a building energy system model through an optimization routine, Appl. Energy 162 (2016) 1010–1023, https://doi.org/10.1016/j.apenergy.2015.10.137.
[8] G.P. Henze, D.E. Kalz, C. Felsmann, G. Knabe, Impact of forecasting accuracy on predictive optimal control of active and passive building thermal storage inventory, HVAC&R Res. 10(2) (2004) 153–178. doi:10.1080/10789669.2004.10391097..
[9] G. Ramos Ruiz, E. Lucas Segarra, C. Fernández Bandera, Model predictive control optimization via genetic algorithm using a detailed building energy model, Energies 12 (1) (2019), https://doi.org/10.3390/en12010034, URL: https://www.mdpi.com/1996-1073/12/1/34.
[10] C. Fernández Bandera, J. Pachano, J. Salom, A. Peppas, G. Ramos Ruiz, Photovoltaic plant optimization to leverage electric self consumption by harnessing building thermal mass, Sustainability 12 (2) (2020), https://doi.org/10.3390/su12020553, URL: https://www.mdpi.com/2071-1050/12/2/553.
[11] J. Reynolds, Y. Rezgui, A. Kwan, S. Piriou, A zone-level, building energy optimisation combining an artificial neural network, a genetic algorithm, and model predictive control, Energy 151 (2018) 729–739, https://doi.org/10.1016/j.energy.2018.03.113.
[12] J.E. Pachano, C.F. Bandera, Multi-step building energy model calibration process based on measured data, Energy Build. 252 (2021), https://doi.org/10.1016/j.enbuild.2021.111380 111380.
[13] G. Chaudhary, J. New, J. Sanyal, P. Im, Z. O'Neill, V. Garg, Evaluation of "autotune" calibration against manual calibration of building energy models, Appl. Energy 182 (2016) 115–134, https://doi.org/10.1016/j.apenergy.2016.08.073.
[14] A. Guideline, Guideline 14-2002, measurement of energy and demand savings, American Society of Heating, Ventilating, and Air Conditioning Engineers, Atlanta, Georgia (2014)..
[15] T. Hong, Y. Chen, X. Luo, N. Luo, S.H. Lee, Ten questions on urban building energy modeling, Build. Environ. 168 (2020), https://doi.org/10.1016/j.buildenv.2019.106508 106508.
[16] Y. Lyu, Y. Pan, T. Yang, Y. Li, Z. Huang, R. Kosonen, An automated process to calibrate building energy model based on schedule tuning and signed directed graph method, J. Build. Eng. 35 (2021), https://doi.org/10.1016/j.jobe.2020.102058 102058.
[17] M. Manfren, N. Aste, R. Moshksar, Calibration and uncertainty analysis for computer models - a meta-model based approach for integrated building energy simulation, Appl. Energy 103 (2013) 627–641, https://doi.org/10.1016/j.apenergy.2012.10.031.
[18] D. Hou, I. Hassan, L. Wang, Review on building energy model calibration by bayesian inference, Renew. Sustain. Energy Rev. 143 (2021), https://doi.org/10.1016/j.rser.2021.110930 110930.
[19] M.H. Kristensen, R. Choudhary, S. Petersen, Bayesian calibration of building energy models: Comparison of predictive accuracy using metered utility data

of different temporal resolution, Energy Procedia 122 (2017) 277–282, cISBAT 2017 International ConferenceFuture Buildings & Districts – Energy Efficiency from Nano to Urban Scale. doi:10.1016/j.egypro.2017.07.322..
[20] C.M. Calama-González, P. Symonds, G. Petrou, R. Suárez, Ángel Luis León-Rodríguez, Bayesian calibration of building energy models for uncertainty analysis through test cells monitoring, Appl. Energy 282 (2021), https://doi.org/10.1016/j.apenergy.2020.116118 116118.
[21] N. Fumo, M.J. Torres, K. Broomfield, A multiple regression approach for calibration of residential building energy models, J. Build. Eng. 43 (2021), https://doi.org/10.1016/j.jobe.2021.102874 102874.
[22] G. Ramos Ruiz, C. Fernández Bandera, T. Gómez-Acebo Temes, A. Sánchez-Ostiz Gutierrez, Genetic algorithm for building envelope calibration, Appl. Energy 168 (2016) 691–705, https://doi.org/10.1016/j.apenergy.2016.01.075.
[23] G. Ramos Ruiz, C. Fernández Bandera, Analysis of uncertainty indices used for building envelope calibration, Appl. Energy 185 (2017) 82–94, https://doi.org/10.1016/j.apenergy.2016.10.054.
[24] A.H. Neto, F.A.S. Fiorelli, Comparison between detailed model simulation and artificial neural network for forecasting building energy consumption, Energy Build. 40 (12) (2008) 2169–2176, https://doi.org/10.1016/j.enbuild.2008.06.013.
[25] S. Karatasou, M. Santamouris, V. Geros, Modeling and predicting building's energy use with artificial neural networks: Methods and results, Energy Build. 38 (8) (2006) 949–958, https://doi.org/10.1016/j.enbuild.2005.11.005.
[26] G. Tardioli, A. Narayan, R. Kerrigan, M. Oates, J. O'Donnell, D.P. Finn, A methodology for calibration of building energy models at district scale using clustering and surrogate techniques, Energy Build. 226 (2020), https://doi.org/10.1016/j.enbuild.2020.110309 110309.
[27] F.S. Westphal, R. Lamberts, Building simulation calibration using sensitivity analysis, in: Ninth International IBPSA Conference, Citeseer, 2005, pp. 1331–1338..
[28] J.C. Lam, S.C. Hui, Sensitivity analysis of energy performance of office buildings, Build. Environ. 31 (1) (1996) 27–39, https://doi.org/10.1016/0360-1323(95)00031-3.
[29] L. Corbusier, P. Jeanneret, Five points towards a new architecture, Programs and manifestoes on 20th-century architecture, MIT Press, Cambridge, 1970, pp. 99–101.
[30] R. Cook, J. Gilbert, The fifth façade: Designing nature into the city, Council on Tall Buildings and Urban Habitat 1 (26) (2015) 288.
[31] V. Gutiérrez González, G. Ramos Ruiz, C. Fernández Bandera, Impact of actual weather datasets for calibrating white-box building energy models base on monitored data, Energies 14 (4) (2021), https://doi.org/10.3390/en14041187, URL: https://www.mdpi.com/1996-1073/14/4/1187.
[32] D.B. Crawley, J.W. Hand, M. Kummert, B.T. Griffith, Contrasting the capabilities of building energy performance simulation programs, Build. Environ. 43(4) (2008) 661–673, part Special: Building Performance Simulation. doi:10.1016/j.buildenv.2006.10.027..
[33] A.-T. Nguyen, S. Reiter, P. Rigo, A review on simulation-based optimization methods applied to building performance analysis, Appl. Energy 113 (2014) 1043–1058, https://doi.org/10.1016/j.apenergy.2013.08.061.
[34] N.J. Kruis, Development and application of a numerical framework for improving building foundation heat transfer calculations, Ph.D. thesis, University of Colorado at Boulder (2015)..
[35] V.G. González, G.R. Ruiz, E.L. Segarra, G.C. Gordillo, C.F. Bandera, Characterization of building foundation in building energy models, Proceedings of the Building Simulation, Rome, Italy (2019) 2–4 doi:10.26868/25222708.2019.210925..
[36] U. EnergyPlus, Department of energy. 2019. input output reference the encyclopedic reference to energyplus input and output (2019)..
[37] G.R. Ruiz, C.F. Bandera, Validation of calibrated energy models: Common errors, Energies 10 (10) (2017), https://doi.org/10.3390/en10101587.
[38] V.G. González, L.Á. Colmenares, J.F.L. Fidalgo, G.R. Ruiz, C.F. Bandera, Uncertainy's indices assessment for calibrated energy models, Energies 12 (11) (2019) 2096, https://doi.org/10.3390/en12112096, URL: https://www.mdpi.com/1996-1073/12/11/2096.
[39] Kiva software,https://bigladdersoftware.com/projects/kiva/ (Accessed: 2021-08-01)..
[40] T. Kusuda, P.R. Achenbach, Earth temperature and thermal diffusivity at selected stations in the united states, Tech. rep., National Bureau of Standards Gaithersburg MD (1965)..
[41] L. Xing, Estimations of undisturbed ground temperatures using numerical and analytical modeling, Ph.D. thesis, Oklahoma State University, copyright - Database copyright ProQuest LLC; ProQuest does not claim copyright in the individual underlying works; Última actualización - 2021-05-25 (2014). URL: https://www.proquest.com/dissertations-theses/estimations-undisturbed-ground-temperatures-using/docview/1661457187/se-2?accountid=14600..
[42] E. DOE, Daylighting calculations: Engineering reference-energyplus 9.0 (2018)..
[43] C. Fernández Bandera, G. Ramos Ruiz, Towards a new generation of building envelope calibration, Energies 10 (12) (2017), https://doi.org/10.3390/en10122102, URL: https://www.mdpi.com/1996-1073/10/12/2102.
[44] V. Gutiérrez González, G. Ramos Ruiz, C. Fernández Bandera, Empirical and comparative validation for a building energy model calibration methodology, Sensors 20 (17) (2020), https://doi.org/10.3390/s20175003, URL: https://www.mdpi.com/1424-8220/20/17/5003.
[45] C.T. de la Edificación, Cte, Disponible en la web: https://www. codigotecnico. org/(Última vez consultado Octubre 2018) (2006)..
[46] Y. Zhang, I. Korolija, Performing complex parametric simulations with jeplus, in: SET2010-9th International Conference on Sustainable Energy Technologies, 2010, pp. 24–27.
[47] K. Deb, A. Pratap, S. Agarwal, T. Meyarivan, A fast and elitist multiobjective genetic algorithm: Nsga-ii, IEEE Trans. Evol. Comput. 6 (2) (2002) 182–197, https://doi.org/10.1109/4235.996017.